ISSN 2176-5480

22nd International Congress of Mechanical Engineering (COBEM 2013)
November 3-7, 2013, Ribeirão Preto, SP, Brazil

EXPERIMENTAL STUDY OF CONVECTIVE INSTABILITY IN FREE JETS

Davi Bernhard de Souza
Instituto Militar de Engenharia - Pós-Graduação em Engenharia de Defesa, Pça. Gen. Tibúrcio, 80, Praia Vermelha, Rio de Janeiro - RJ, 22290-270, Brasil.
davibernhard@gmail.com

Leonardo Santos de Brito Alves
Universidade Federal Fluminense, Centro Tecnológico, Escola de Engenharia, R. Passo da Pátria n. 156, bloco E, sala 216, São Domingos, Niterói - RJ, 24210-240, Brasil.
leonardo.alves@gmail.com

Maria Helena Farias
Divisão de Metrologia em Dinâmica de Fluidos - DINAM/ Diretoria de Metrologia Científica e Industrial - DIMCI, INMETRO, Av. Nossa Senhora das Graças, 50, prédio 06, Xerém - Duque de Caxias - RJ, 25250-020, Brasil.
mhfarias@inmetro.gov.br

Abstract. *Hot-wire anemometry data for the instantaneous velocity profile of a jet issuing from a convergent nozzle is obtained in order to extract its frequency spectrum and spatial growth rates for different Reynolds numbers. Comparisons are performed with linear stability analysis for validation purposes. Critical parameters for the convectively unstable region are determined. This study represents a preliminary investigation and validation of the experimental setup. Both theoretical and experimental analyzes will be extended to an axisymmetric coaxial nozzle configuration to evaluate the effects of blowing and suction control using the outer nozzle. Such a study has already been performed in the literature and will be used to validate the experimental setup. After both validation steps have been performed, this coaxial jet setup will be extended to study elliptic nozzles.*

Keywords: *axisymmetric nozzle, hot-wire, velocity profile, experimental, convective instability.*

1. INTRODUCTION

The ultimate goal of the present research project is the study of coaxial elliptic jets. Our final objective is to analyze how the inner jet instability under blowing or suction through the outer nozzle is affected by the coupling between different modes introduced by the elliptic geometry. Its convective instability as well as its onset of absolute instability are going to be investigated. As far as the authors are aware, such a research is yet to be presented in the literature. The present study, an experimental analysis of convective instability in free jets generated by convergent nozzles, represents the first step towards this goal. Hence, the short literature review presented next is focused on free jets.

Batchelor and Gill (1962) were among the first to study free jets. They used a linear and inviscid stability analysis based on a local and parallel base flow, whose velocity profile was modeled as a cylindrical vortex sheet. Temporal and (spatial) growth rates were found to increase monotonically with respect to the wave number (frequency). This lack of a maximum is unrealistic, but is a common feature of discontinuous profiles and a good approximation for continuous profiles for small wave numbers (frequencies). Michalke (1971) extended this study by considering a hyperbolic tangent function as a model for the continuous velocity profile of a free jet. He found a finite range of unstable frequencies containing a maximum in spatial growth rate. Furthermore, both range and maximum increased by decreasing the jet mixing-layer momentum thickness. These results are in good agreement with the experimental data obtained by Crow and Champagne (1971), who introduced the concept of a coherent structure and showed that turbulence could be viewed as a superposition of vortices of different scales. Many years later, Hussain (1986) became one of the first to use active control for free jets. He employed acoustic excitation to act directly on axisymmetric perturbations present at the nozzle exit in order to guide the formation of the resulting coherent structures. Corke and Kusek (1993), extended this study by considering acoustic excitation of helical modes instead. Finally, Strykowski and Wilcoxon (1993) introduced the concept of passive control using an outer nozzle to introduce blowing and suction. Instead of acting directly on the perturbation amplitude through active control, their approach modifies the base flow that feeds energy to the existing perturbations, indirectly controlling the formation of coherent structures.

2. DESCRIPTION OF THE EXPERIMENT

2.1 Layout

As shown in Fig. 1, the layout used on this experiment had a frequency inverter to control the fan rotation and hence, the induced flow speed, i.e. the air mass flow rate provided the nozzle. After the inverter there is a pipe connected to an elbow and another pipe. After this there is a sequence of devices: a screen, a hive and another screen, in

ISSN 2176-5480

order to minimize the turbulence intensity of the air flow generated by the fan. The use of a screen is described in detail by Soltani, *et al.* (2010). The hive used in this study was made of small straws.

After this section of the injection system, another pipe is included to allow the flow to become fully developed. The nozzle in attached to the end of this pipe, where its specifications can be seen in Fig. 2. A fifth order polynomial was employed to create the cross section area variation along the stream wise direction inside the nozzle. A smooth entry and exit were considered by imposing zero derivatives in this polynomial for each location.

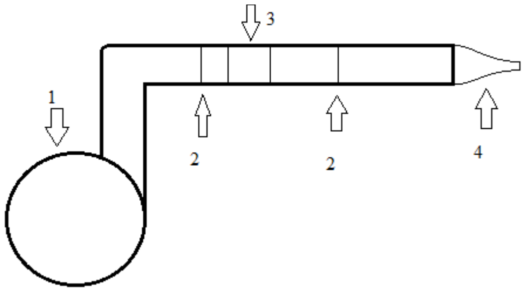

Figure 1 - Layout of the measurement. 1 - fan, 2 - screens, 3 - hive, 4 - nozzle.

In order to minimize any vibrations from the lab coming through the ground, vibra-stops were used in the supporting structure that holds the pipes forming the horizontal part of the injection system in this figure. Furthermore, the vertical pipe that connects this part to the fan is made of cloth to minimize vibrations from the fan. The hot-wire transverse system also has a vibra-stop to minimize vibrations.

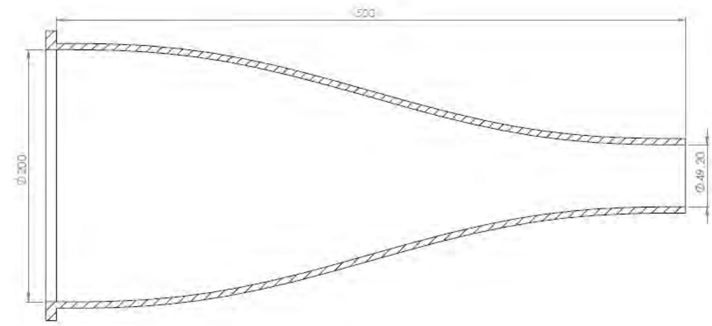

Figure 2 - Nozzle used to generate top-hat free jet.

This convergent nozzle is made of glass fiber. It was manufactured according to the following process: First, a mold was created in wood using a CNC machine. Then, this mold was covered with glass fiber, using resin to make the internal surface smooth. This method will cause some small differences when compared to a CNC crafted nozzle.

Hot-wire velocity calibration was performed using a pitot tube attached to a barometer. The software used is the StreamLine from Dantec. An explanation of the anemometry measurement is described in the next subsection. All data was post-processed using the software Mathematica, where plots and their analysis is shown in section 3.

2.2 Anemometry systems

A hot-wire anemometer was chosen as the main data acquisition system for this work. It has the highest acquisition rate among its counterparts and can be very precise if correctly calibrated. The functioning principle of the hot-wire is quite simple. The program works with a Wheatstone bridge, a probe and a wire, which works as one of the resistances. As the current passes through the wire, it will dissipate heat to the fluid. In order to maintain the temperature constant in the probe, the program allows more current to the bridge, which changes the voltage. A polynomial or exponential equation can be used to fit the voltage data as a function of the temperature, which can now be correlated the velocity of the fluid in which the probe is immersed. However, in order to acquire the adjustable coefficients for this equation, calibration is required.

In order to calibrate the system, a separate equipment must be able to provide the correct value for the velocity. So, once the inverter is set to a certain frequency, the pitot tube and the barometer measure the velocity at a corresponding voltage value. Given enough points for a good polynomial regression, the StreamLine software yields the best fit and saves that result, so interpolation can be employed at different voltages to yield a velocity measurement.

ISSN 2176-5480

Even with a more accurate system to collect the velocity for the calibration, there will still be some errors associated to these measurements, mostly caused by frequency disturbances. More details are provided by Both Yavuzkurt (1984) and Santos, *et al.* (2006), who discuss how error in calibration curves affects measurements.

3. DATA ANALYSIS

Figure 2 shows the nozzle with the specifications to assemble it, which were: length *L=500 mm*, diameter at the entrance *D=200 mm* and at the exit *d=49,2 m*. The experiment was performed inside a laboratory with constant ambient temperature at approximately *24 °C*. This temperature was also acquired by the software StreamLine and used to compensate the velocity measurements. Data was acquired using a sample extraction rate of *10000 Hz*, where the total number of samples is *16384*.

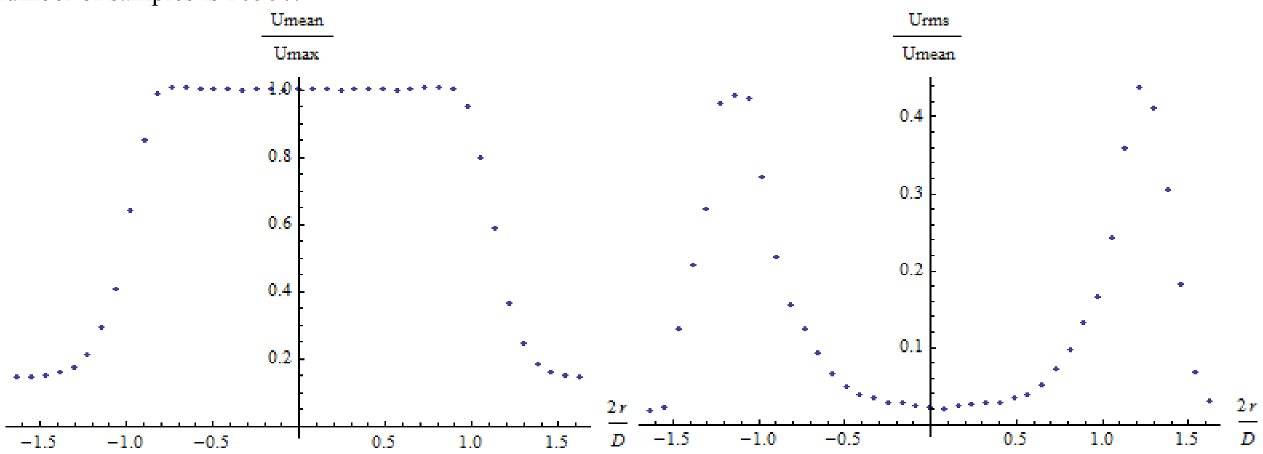

Figure 3 – Mean and rms velocity profiles at *x/d=1*.

The Reynolds imposed for the experiment was as low as possible, with its lower limit restricted by the inverter's ability to operate at such low frequencies. This dimensionless parameter was calculated using the traditional definition

$$Re_d = \rho U d / \mu \quad (1)$$

where *d* is the exit diameter of the nozzle, *U* is the maximum jet velocity, and the μ/ρ is the kinematic viscosity of the fluid, which is air in the present case. The minimum frequency that the inverter could maintain the fan operating was approximately *6 Hz*. This allowed data to be acquired with $Re_d = 36000$, *12000*, and *6000*, where the last value has an associated frequency very close to the operational limit that the inverter can maintain. If the nozzle had a smaller exit diameter, the Reynolds could be lower for the same frequency imposed by the inverter.

Samples were taken in five different positions, which were kept the same for all three values of Re_d analyzed. All these positions are given in terms of the length in the *x* coordinate measuring the distance to the nozzle exit. They are *x/d = 0.1, 1, 2, 3* and *4*. This data is expected to have the form of a top hat profile near the nozzle exit but tends to the traditional similarity profile further downstream. As Re_d increases, the turbulent intensity also increases but the jet spread, indirectly measured through the mixing-layer thickness, decreases. Hence, the expected form of these curves might not be the same between different cases.

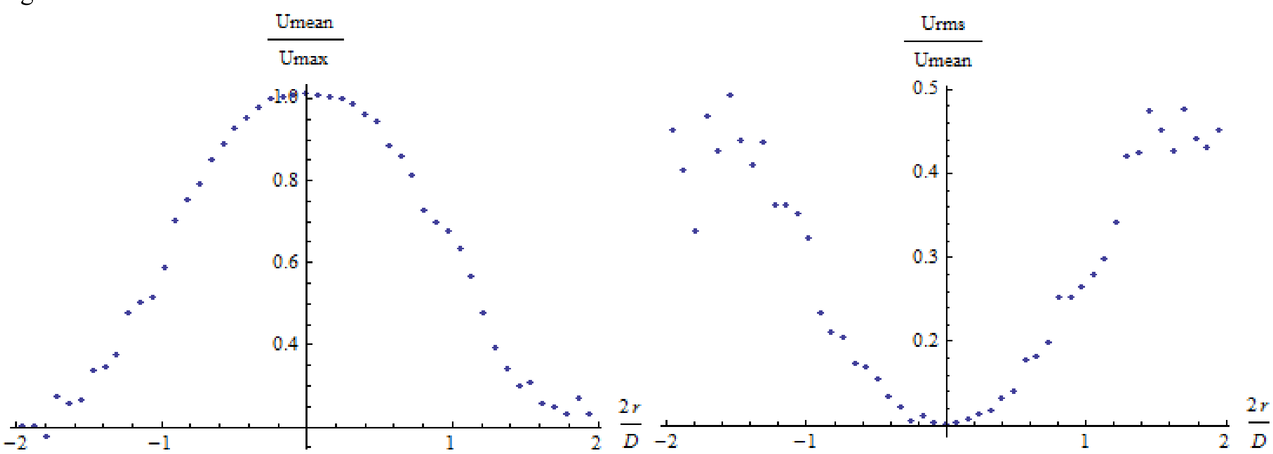

Figure 4 - Mean and rms velocity profiles at *x/d=4*.

ISSN 2176-5480

The root mean square value of the velocity, or the corrected sample standard deviation of the velocity, was also obtained. It is presented in a dimensionless form, divided by the mean velocity. This variable is expected to be higher where the turbulence intensity is higher. It is well known that this is true within the mixing-layer region, where the free jet vorticity is concentrated.

3.1 Data analisys at *Re* = *36000*

Figure 3 shows the results for the mean velocity $U_{med} = 11{,}06\ m/s$, which corresponds to the Re_d in this subsection title. The left-hand-side plot in this figure shows the mean velocity data measured in forty-one points whereas the right-hand-side plot in this figure shows the rms velocity at the same points. This data was obtained at *x/d=1*, i.e. near the jet exit. On the other hand, Fig. 4 show the same plots, but at *x/d=4*. The data in this figure was measured in fifty-five points instead, because of the flow spread.

As can be seen in both figures, the measurements agree with the theory, which states that the velocity profile has a top-hat form and its rms has the highest value near the nozzle wall location ($r \sim d/2$), since the convergent nozzle reduces the boundary-layer thickness of the flow inside of it, effectively reducing the jet mixing-layer.

Further downstream of the nozzle exit, Fig. 4 shows similar results, but at *x/d=4*. They compare well to the results shown above, with a similar qualitative behavior, except with a thicker mixing-layer. It is also noticeable that this distance is close to the end of the potential core, where the mixing-layer spread reaches the jet centerline. The amount of noise in this figure is also a little higher, probably due to the longer turbulent region.

3.2 Data analisys at *Re* = *12000*

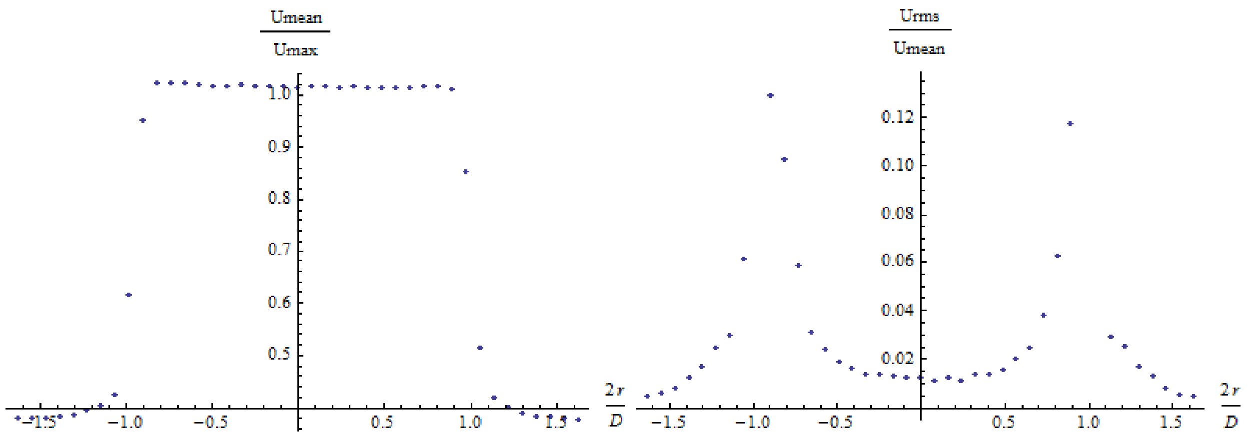

Figure 5 - Mean and rms velocity profiles at *x/d=1*.

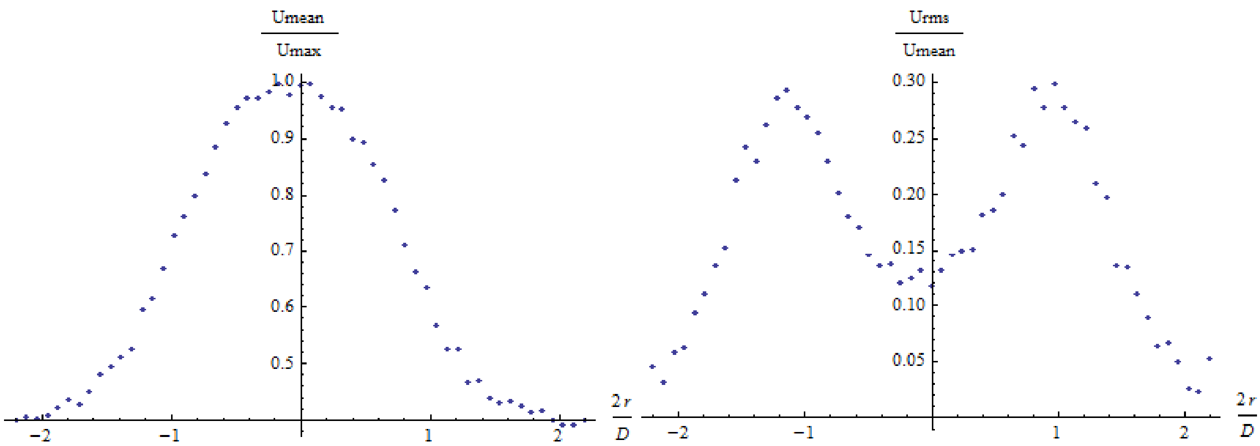

Figure 6 - Mean and rms velocity profiles at *x/d=4*.

Figure 5 shows the results for a velocity of $U_{med} = 3{,}69\ m/s$. It follows the same outline shown in Fig. 3. Note that the mixing-layer thickness has decreased, probably due to the significant decrease in turbulence intensity, observed through the smaller rms velocity. This means perturbations at the jet exit have smaller amplitude, which delays the

ISSN 2176-5480

formation of the coherent structures known as vortices. Figure 6 also resembles Fig. 4, except that *x/d=4* is much closer to the end of the potential core, since the rms velocity is proportionally higher at the centerline.

3.3 Data analisys at *Re = 6000*

Figure 7 shows the results for the velocity of U_{med} = *1,84m/s*. Once again the same behavior observed at *x/d=1* in Figs 5 and 4 are observed here. The velocity rms decreased even further, continuing the trend of a smaller mixing-layer thickness due to smaller perturbation amplitudes at the jet exit.

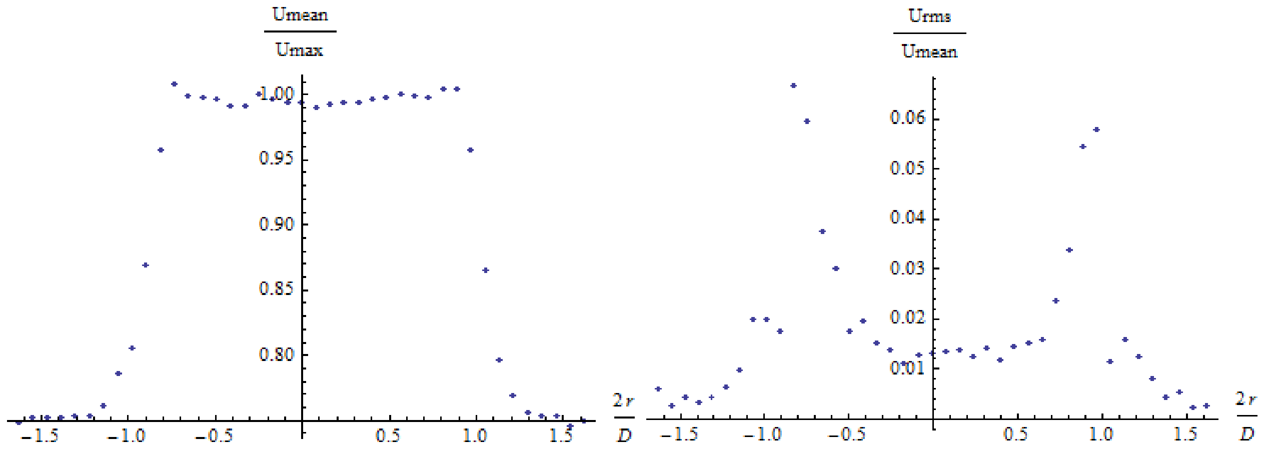

Figure 7 - Mean and rms velocity profiles at *x/d=1*.

This trend manifests very clearly in Figure 8, since the velocity rms is higher at the jet centerline when *x/d=4*. This is a very strong indication that the potential core has ended at this location.

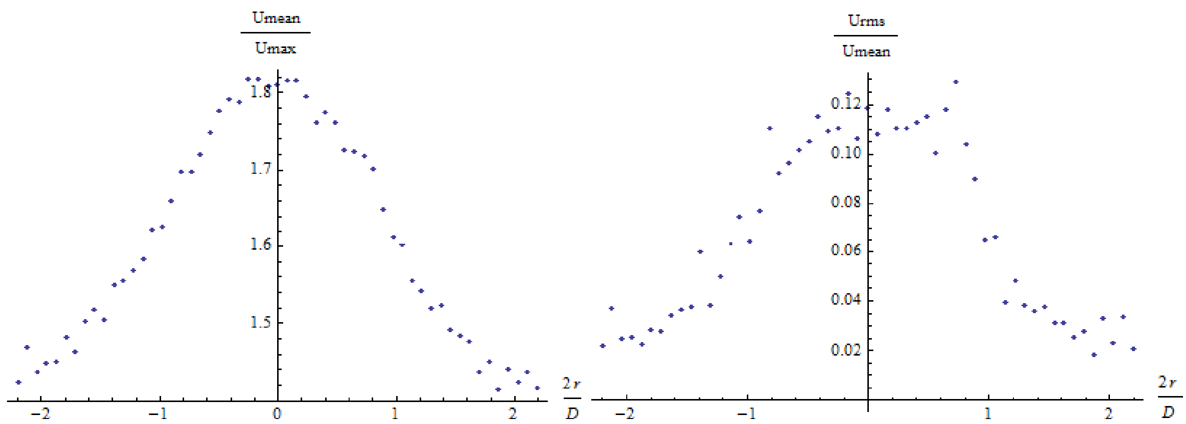

Figure 8 - Mean and rms velocity profiles at *x/d=4*.

4. CONCLUSIONS AND FUTURE WORK

As the Reynolds number decreases, the amplitude of the perturbations present at the nozzle exit also decreases. Hence, the convectively instability process that creates vortex structures is delayed.

There are still several problems with the present experimental data. The reasons diagnosed so far are: 1) sample size is too small, which is the most likely cause for the non-smooth behavior of the data points, 2) homogenous distribution of measured points, which leads to a poor description of the mixing-layer region, 3) absence of an isolation system for the experiment, which explains why the measured velocity profile does not go to zero away from the jet centerline.

5. REFERENCES

BATCHELOR, G. K. & Gill, A. E. *Analysis of the stability of axisymmetric jets*. Journal of Fluid Mechanics 14, 529–551. 1962.

BRUUN, H. H. *Hot-Wire Anemometry: Principles and Signal Analysis*. Oxford University Press, 1995.
CORKE T. C. and KUSEC S. M., Resonance in axisymmetric jets with controlled helical-mode input. J. Fluid Mech. 249, pp. 307, 1993.
CROW, S. C. & CHAMPAGNE, F. M. *Orderly structure in jet turbulence*. Journal of Fluid Mechanics, 48:547-591, 1971.
HUSSAIN, A. K. M. F. *Coherent structures and turbulence*. Journal of Fluid Mechanics, vol 173, p. 303–356. 1986.
MICHALKE, A. *Instabilität eines Kompressiblen Runden Freistrahls unter Berücksichtigung des Einflusses der Strahlgrenzschichtdicke*. Zeitschrift für Flugwissenchaften, vol 19, no 8-9, pp 319–328, 1971.
SANTOS, L. A., REIS, M. L. C. C., MELLO, O. A. F., MEZZALIRA, L. G. *Propagation of uncertainties in the calibration curve fitting of single normal hot-wire anemometry probes*. XVIII IMEKO World Congress, Rio de Janeiro 2006.
SOLTANI, M. R., GHORBANIAN, K., MANSHADI, M. D. *Application of screens and trips in enhancement of flow characteristics in subsonic wind tunnels*. Mechanical Engeneering, vol 17, n° 1, p. 1-12. 2010.
STRYKOWSKI, P. J. & WILCOXON, R. K. *Mixing enhancement due to global oscillations in jets with annular counterflow*. AIAA Journal, 31(3):564-570, 1993.
YAVUZKURT, S. *A guide to uncertainty analysis of hot-wire data*. Journal of Fluids Engineering, vol 106, p. 181-186. 1984.

6. RESPONSIBILITY NOTICE

The authors are the only responsible for the printed material included in this paper.